CrossMark

Reverse osmosis issues relating to pressure drop, mass transfer, turbulence, and unsteadiness

G. Srivathsan, Eph M. Sparrow *, John M. Gorman

Department of Mechanical Engineering, Laboratory for Engineering Practice, University of Minnesota, Minneapolis, MN 55455, USA

HIGHLIGHTS

- Flow regimes, flow unsteadiness, periodicity model, membrane surface condition
- Parameters' feed spacer thickness and strand angle, strand spacing, strand radius
- Algebraic correlations of pressure drop and mass transfer Sherwood number
- Turbulence nondetectable and unsteadiness too small to affect the results
- Streamwise periodicity of the fluid flow was verified.

ARTICLE INFO

ABSTRACT

Numerical simulation has been used to investigate a number of significant physical processes for reverse osmosis in a spiral-wound membrane, including fluid-flow regimes, flow unsteadiness, and fluid-flow periodicity. The independent variables included the feed spacer strand angle, feed spacer thickness, inter strand spacing, strand radius, radius of the center cylinder, and Reynolds number. Results extracted from the numerical solutions were post-processed to provide algebraic correlations for both the dimensionless pressure drop and the Sherwood number. For the range of Reynolds numbers relevant to practice, turbulence was found to be nonexistent. Flow unsteadiness was identified for certain ranges of the Reynolds number and the geometrical parameters. The extent of the unsteadiness was sufficiently moderate so as not to have any practical effect on the dimensionless pressure drop and Sherwood number. Fluid-flow periodicity was verified.

© 2014 Elsevier B.V. All rights reserved.

1. Introduction

Recent concerns about worldwide water insufficiencies have spurred interest in means of converting non-potable water into water suitable for human consumption. All present conversion means are energy-utilizing. As a consequence, the current literature has focused on increasing the efficiency of conversion. The work reported here continues that process. Focus is directed to reverse osmosis, which is presently the most used means of converting naturally available non-potable water. The novel features relevant to reverse osmosis that are investigated here are: (a) development of encompassing dimensionless correlations for pressure drop and for mass transfer, (b) assessment of flow regimes (laminar, intermittent, or turbulent), (c) modeling of unsteady flow versus steady flow, and (d) membrane surface boundary

conditions. The correlation work revealed some yet unresolved disparities that place present design methods in some uncertainty.

Numerical simulation is used to analyze the flow through the feed spacers of spiral-wound reverse osmosis membrane elements. The geometrical model adopted here is similar to that of Fimbres-Weihs and Wiley [1], but with the exception that in the present model, each fiber crossing is enveloped in a thin cylindrical sheath as shown in Part (a) of Fig. 1. This innovation was incorporated after careful observations of numerous crossings by means of an optical microscope. In the opinion of the authors, this geometric feature should not have a significant effect on the results. A schematic diagram of the solution domain is displayed in Fig. 1(b). In particular, the solution domain is the space enclosed within the rectangular boundary.

The geometrical periodicity of the problem is clearly evident but fluid-flow periodicity awaits verification. To this end, the velocity normal to the membrane wall was set to a realistic value, and a numerical solution was implemented for this condition. The outcome was compared to that obtained for the conventional treatment of the membrane wall (zero normal velocity), and the difference was 0.145%.

* Corresponding author. Tel.: +1 612 625 9881.
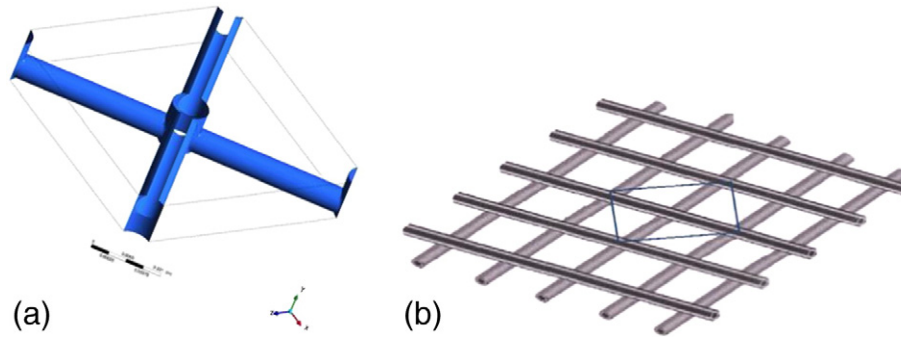 *E-mail address:* esparrow@umn.edu (E.M. Sparrow).

Fig. 1. (a) Fiber-crossing configuration and (b) definition of the solution domain.

2. Numerical simulations

The numerical simulations were performed for a range of Reynolds numbers from 50 to 500, where the Reynolds number is defined as

$$Re = \frac{\rho U d_h}{\mu} \tag{1}$$

in which ρ and μ are, respectively, the density and viscosity of the flowing liquid, U is the mean fluid velocity, and d_h is the hydraulic diameter. The latter is equal to twice the feed spacer channel height. Although the Reynolds numbers in the investigated range might be regarded as strictly laminar when viewed with respect to simple pipe flow knowledge, the geometry of the feed channel is distinguished by a roughness-like surface which might give rise to turbulence or intermittency at the highest values of the Reynolds number. This issue will be among those to be investigated. The working fluid was a mixture of pure water and 2000 ppmw of sodium chloride with a density of 997 kg/m^3, viscosity of 8.89×10^{-4} kg/m-s, and diffusion coefficient of 1.5×10^{-9} m^2/s.

Other parameters to be considered in the numerical simulations are: (a) feed spacer strand angle, (b) feed spacer thickness, (c) feed strand spacing, (d) feed strand radius, (e) radius of center cylinder, and (f) pressure difference driving the feed flow. For the numerical simulations to be reported here, the values of the foregoing quantities are: (a) 90°, (b) 0.508 to 0.889 mm, (c) 2.54 mm, (d) 0.145 to 0.254 mm, (e) 0.206 to 0.361 mm, and (f) adjusted to give rise to the aforementioned range of Reynolds numbers.

The numerical solutions were implemented by means of the ANSYS CFX 14.0 software package. The three-dimensional Navier–Stokes equations, the equation of continuity, and the species conservation equation for salt were solved simultaneously for laminar flow. For the investigation of turbulent flow, a turbulence model, the Shear Stress Transport model, was implemented. That turbulence model was chosen because it auto-corrects the intensity of turbulence depending on the actual flow regime. The numerical work was performed with the governing equations in dimensional form.

Solutions were carried out for both steady and unsteady operating conditions. The case of turbulent flow was performed as a diagnostic activity rather than as a full-blown evaluation, as was the solution for unsteady-state operation. The discretizations of the solution domain yielded meshes consisting of nodal numbers ranging from approximately one million to two and a half million. Mesh independence was tracked by monitoring the values of the dimensionless pressure drop, Eq. (3), as a function of the number of nodes in the solution domain. When changes in the dimensionless pressure drop diminished to approximately 0.1% for an incremental change of 10,000 nodes, the solution was accepted.

3. Correlation of pressure drop results

It is common to represent the feed spacer pressure drop in terms of a dimensionless quantity termed the Power number Pn. Since the composition of the Power number is not universal, it is necessary to state the definition used here, which is

$$Pn = \left(-\frac{dp}{dx}\right)\frac{\rho^2}{\mu^3}U h^4 = \frac{1}{32}f Re^3 \tag{2}$$

where

$$f = \left(-\frac{dp}{dx}\right)\frac{d_h}{\frac{1}{2}\rho U^2} \tag{3}$$

and Re, ρ, μ, U, and d_h have been defined in connection with Eq. (1). In addition, p is the static pressure, x is the direction of the flowing fluid, f is the friction factor, and h is the feed spacer channel height (half of d_h).

The Pn results extracted from the present simulations are plotted in Fig. 2 along with the results from [1] and [2] which were also obtained numerically. Inspection of the figure indicates a common trend which shows the Power number increasing monotonically with the Reynolds number. The rate of increase is greatest in the lower Reynolds number range and decreases with increasing values of the Reynolds number. Overall, the agreement among three sets of results is satisfactory, especially for the comparison between the present results and those of [2]. In the range of higher Reynolds numbers, the comparison displayed in Fig. 2 is better than similar comparisons made elsewhere [5].

The totality of pressure drop information extracted from the present numerical simulations is extensive because of the numerous parameters
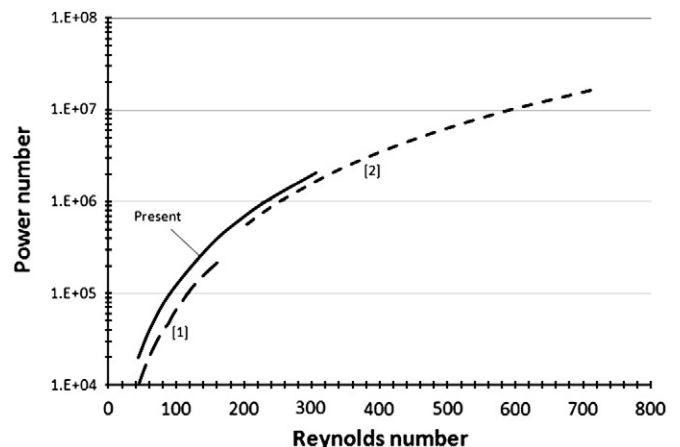

Fig. 2. Comparison of power number results.